



LAWRENCE  
LIVERMORE  
NATIONAL  
LABORATORY

# Qualification of the Joints for the ITER Central Solenoid

N. Martovetsky, A. Berryhill, S. Kenney

September 2, 2011

MT-22 Magnet Technology Conference  
Marseille, France  
September 12, 2011 through September 16, 2011

## **Disclaimer**

---

This document was prepared as an account of work sponsored by an agency of the United States government. Neither the United States government nor Lawrence Livermore National Security, LLC, nor any of their employees makes any warranty, expressed or implied, or assumes any legal liability or responsibility for the accuracy, completeness, or usefulness of any information, apparatus, product, or process disclosed, or represents that its use would not infringe privately owned rights. Reference herein to any specific commercial product, process, or service by trade name, trademark, manufacturer, or otherwise does not necessarily constitute or imply its endorsement, recommendation, or favoring by the United States government or Lawrence Livermore National Security, LLC. The views and opinions of authors expressed herein do not necessarily state or reflect those of the United States government or Lawrence Livermore National Security, LLC, and shall not be used for advertising or product endorsement purposes.

# Qualification of the Joints for the ITER Central Solenoid

Nicolai N. Martovetsky, Adam B. Berryhill, and Steve J. Kenney

**Abstract**—The ITER Central Solenoid has 36 interpancake joints, 12 bus joints, and 12 feeder joints in the magnet. The joints are required to have resistance below 4 nOhm at 45 kA at 4.5 K. The US ITER Project Office developed two different types of interpancake joints with some variations in details in order to find a better design, qualify the joints, and establish a fabrication process.

We built and tested four samples of the sintered joints and two samples with butt-bonded joints (a total of eight joints). Both designs met the specifications.

Results of the joint development, test results, and selection of the baseline design are presented and discussed in the paper.

**Index Terms**— multifilamentary superconductors, Superconducting cables, superconducting magnets, superconducting transformers.

## I. INTRODUCTION

THE ITER Central Solenoid (CS) consists of six modules. Each module is composed of six wound hexapancakes and one quadrapancake. The multipancakes are connected electrically and hydraulically by in-line interpancake joints. The joints are located at the outside diameter (OD) of the module. Cable in conduit conductor (CICC) high-current joints are critical elements in the CICC magnets. In addition to low resistivity, the CS joints must fit a space envelope equivalent to the regular conductor cross section and must have low hydraulic impedance and enough structural strength to withstand the hoop and compressive forces during operation, including cycling. This paper is the continuation of the work reported on the intermodule joints [1].

## II. INTERPANCAKE JOINT OPTIONS

### A. Butt Joint Design Description

The butt joint, initially a baseline for the CS interpancake, is described in detail in [1]. It is made by diffusion bonding of

Manuscript received 12 September 2011. This work performed under the auspices of the U.S. Department of Energy by Oak Ridge National Laboratory under contract DE-AC05-00OR22725 and by Lawrence Livermore National Laboratory under Contract DE-AC52-07NA27344.

N. N. Martovetsky is with Lawrence Livermore National Laboratory, on assignment to Oak Ridge National Laboratory, USIPO, 1055 Commerce Park, Oak Ridge, TN, 37831 USA, phone 865-576-2100, fax 865-574-8393, e-mail: [martovetskyn@ornl.gov](mailto:martovetskyn@ornl.gov).

A. B. Berryhill is with Cryomagnetics, Inc., Cryomagnetics Inc., 1006 Alvin Weinberg Drive, Oak Ridge, TN 37830, USA [aberryhill@cryomagnetics.com](mailto:aberryhill@cryomagnetics.com).

S. J. Kenney is with ORNL, ORNL 1055 Commerce Park Dr, Oak Ridge, TN 37831 USA, [kenneys@usiter.org](mailto:kenneys@usiter.org).

two cables, highly compacted in a copper sleeve and heat-treated in a vacuum chamber under high contact pressure and at high temperature. The joining parts are cut square, polished, and aligned before joining. Several samples of the butt joint are shown in Fig. 1.



Fig. 1. Butt joints samples for mechanical characterization.

We fully developed the joint-fabrication technology, made sure by metallographic studies that the full surface of the joint was bonded, characterized mechanical properties, and, in the late fall of 2010, measured electrical resistance of four joints.

### B. Sintered Joint Design

The sintered joint was developed in order to mitigate the fabrication risks associated with the butt joint. We modified the EDIPO joint concept proposed by the ENEA Frascati group [2]. A sintered joint option is shown in Fig. 2. It is assembled from six subcables from each side and therefore is called “6 × 6.” Half of the subcables of the last but one stage of the connecting subcables is cut so that the finished joint will not be thicker than the cable. In contrast to the butt joint, the sintered joint is not as tightly compacted and has helium in the cable space and in a central channel all the way through. We also tried a more primitive and simple version, called the “three fingers” design, or 3 × 3, where every other subcable of the last stage was completely cut from both sides and reassembled in a full cable cross section.



Fig. 2. Sintered 6 × 6 joint.

We developed all the procedures and tooling necessary for the fabrication of the joint and studied effect of oxidation on sintering between the strands and to the copper sleeve.

We discovered that extended exposure to a humid atmosphere oxidizes the strands significantly, but during heat treatment in an inert atmosphere, the pure metal surface is restored and the copper surface forms a good sintered bond with other strands and the copper sleeve.

In the sintered joint design, we also addressed the optimal configuration of the subcables in the reassembled cable. The cabling pattern of the CS cable is such that the last stage contains six subcables and last but one – four subcables [3]. There are choices regarding how one can reassemble the cables in the joint. The options are shown schematically in Fig. 3. The optimal configuration of the subcables would be theoretically the interleaved one, on the left, because it has about twice the surface contact between the subcables in the joint. The only advantage of the parallel configuration is that it is a little easier to handle and assemble.



Fig. 3. Two possible arrangement of the last-stage subcable in the sintered joint: on the left, interleaved; on the right, parallel.

We tested both configurations of the joint; both configurations were very close in resistance.

### III. TESTING OF THE JOINTS IN RACETRACK SAMPLES

We built a joint test apparatus (JTA) for testing the joints in the racetrack configuration [1]. It is a transformer with a primary winding inside the test article. Figure 4 shows the sample secured over the primary coil for testing the joints.

In order to measure the current in the racetrack, we measure the magnetic field in two locations with Hall probes, one located in a specified location between the primary coil and the test racetrack (H1) and another one outside of the racetrack (H2).

The contributions to the magnetic field detected by the Hall probes H1 and H2 can be expressed by the following equations:

$$\begin{aligned} H_1 &= k_{p1}I_p + k_{s1}I_s \\ H_2 &= k_{p2}I_p + k_{s2}I_s \end{aligned} \quad (1)$$

where,  $I_p$  and  $I_s$  are the currents in the primary and the sample, respectively. The “ $k$ ” coefficients can be calculated from field analysis by TOSKA, ANSYS, or other codes from known geometry and from the number of turns in the primary.

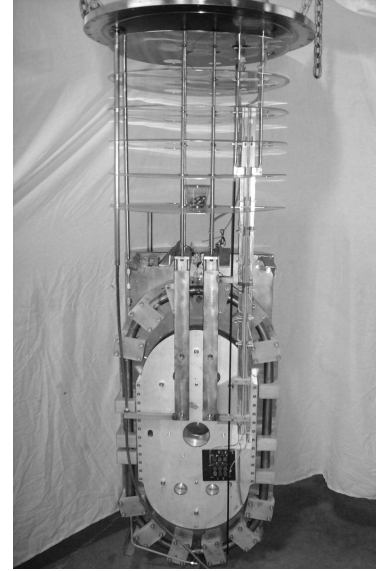


Fig. 4. A racetrack sample prepared for electrical testing.

The easiest way to measure resistance is to measure decay of the magnetic field in the sample while keeping the current in the primary constant after inducing a current in the sample.

The key is to obtain a signal function, by combining the data from H<sub>1</sub> and H<sub>2</sub> that carries only the decay signal from the sample. In other words, we need to cancel the signal from the primary. In many magnets, it is easy to do with a heater that keeps the sample in the normal state and the current in the sample at zero when the primary is energized. Then, before the discharge, the heater is turned off and the current in the primary is discharged to zero. Both Hall probes will read only the signals from the sample current decay. In order to keep the sample in the normal state, our configuration required more power for the heater than we could provide. So we had to live with non-zero current in the primary. Knowing the  $k_{p1}$  and  $k_{p2}$  coefficients, we could easily build a function  $F(I_s)$  from (1) to eliminate the signal from  $I_p$  and thus obtain a clean signal that carried decay of  $I_s$  only:

$$F(t) = (k_{p2}k_{s1} - k_{p1}k_{s2})I_s(t) \quad (2)$$

Resistance of the loop is then calculated from the exponential decay time constant  $\tau$ :

$$R = \frac{L}{\tau} \quad (3)$$

where  $R$  is resistance of the racetrack,  $L$  is computed inductance of the racetrack, and  $\tau$  is the measured exponential decay time.

In addition to the inductive method of the joint measurements, we had a direct voltage measurement across the joint. This direct method is known to be unreliable in the vicinity of the joints because the distribution of the potential around low-resistivity joints may be very nonuniform, and typically the reading of the voltage across the joint gives much lower resistance than could be verified by an inductive method or by a calorimetric method. However, sometimes it comes

close and gives an assurance, especially if the voltage taps are far enough from the joints. Resistance measurement by decay is more reliable than measurement by voltage taps.

Figure 5 shows results of the eight joints (six racetracks) measured in the JTA.

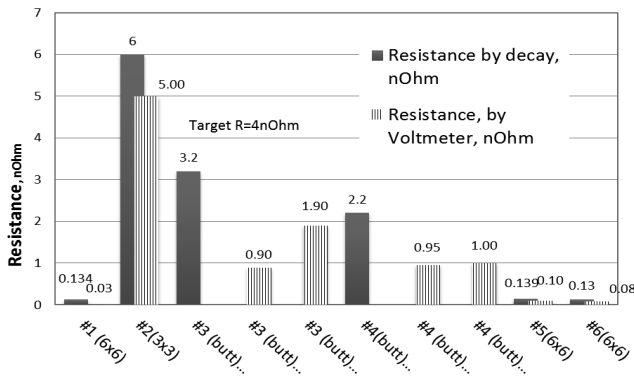


Fig. 5. Summary of the joint resistance measurements.

The  $6 \times 6$  sintered joints all consistently showed a very low resistance of 0.13 nOhm. Racetrack 1 had the subcables arranged in the parallel configuration, as shown in Fig. 3 on the right. Racetracks 5 and 6 had the interleaved arrangements, shown in Fig. 3, on the left.

Resistance of the  $6 \times 6$  sintered joints seems to be insensitive to the arrangement of the subcables, which is counterintuitive.

The butt joint racetracks had two joints in the racetrack; therefore, resistance of the individual joints could not be found by the induction method. Direct voltage measurements of joint resistance have a lower error in the butt joint than in the sintered joint because the current transfer is well defined and distribution of the voltage is more uniform. As we can see from Fig. 5, resistance of the full Racetrack 3 measured by the inductive method is 3.2 nOhm. The individual resistances of the joints measured by a voltmeter and currents measured by Hall probes (0.9 nOhm and 1.9 nOhm) are in approximate agreement for this kind of measurement. Racetrack 4, with two butt joints, has a little closer match: 2.2 nOhm from inductive measurements and 1 and 0.95 nOhm from voltage measurements.

The Racetrack 2, with  $3 \times 3$  subcables, has by far the worst joint resistance. This may in part be because we intentionally tried to connect the subcables to the other ones rather than to each other.

The  $3 \times 3$  joints have every other subcable cut. Therefore, in the  $3 \times 3$  racetrack, there are two possibilities. First, we cut the same subcables from both ends and connect the remaining subcables to each other. In that case, only three subcables participate in current carrying and transfer; the rest have no reason to receive any current until current-carrying capacity limit in the subcables is reached and the generated voltage pushes the current into the neighboring subcable. However, the current-carrying capacity of the subcables is too high in the joints, both in the JTA and in the real CS. Such a situation is dangerous for the real conductor because it generates a

major built-in nonuniformity that may lead to a very low stability for the conductor. In order to avoid such a situation, the subcables at the ends (where the joints are) must be connected to the other subcables so that the current will be forced to occupy all subcables away from the joints. We reproduced this situation and connected different subcables at the ends of the Racetrack 2. That made resistance of the joints a little higher than would be the case in the real CS module, where distribution length is much longer.

We discovered that fabrication of  $6 \times 6$  joints is not much different from fabrication of  $3 \times 3$  joints and therefore there is no reason to use  $3 \times 3$ .

Although we developed the butt joint technology and tooling, and the butt joint was demonstrated to be acceptable from all aspects of fabrication and performance, we chose the  $6 \times 6$  sintered joint for the ITER CS because of its lower risk and simplicity of fabrication.

#### IV. HYDRAULIC STUDIES OF THE SINTERED JOINT

One of the requirements for the hydraulic impedance of the joint is that the impedance would not be more than 5% of the total pressure drop across the hydraulic path in the CS. In order to verify low-pressure impedance, we developed a model of the joint that included the compacted cable, a central channel, and outside grooves machined in the jacket, providing an additional flow channel for helium. We also modeled the ends of the subcables that were TIG welded and fused together at the strand ends in order to prevent leakage of tin from the strands during heat treatment. Because we are planning to use bronze rout strands in the CS conductor, this additional obstacle to the flow will not be there.

The flow distribution in the joint components is shown in Table 1.

TABLE 1 FLOW DISTRIBUTION IN THE SINTERED JOINT AND IN REGULAR CONDUCTOR, g/s

| Location             | Cable space | Central channel | Outside grooves |
|----------------------|-------------|-----------------|-----------------|
| CICC away from joint | 5.1         | 2.9             | n/a             |
| In the joint area    | 1.81        | 2.72            | 3.47            |

Naturally, there is a lower flow in the more compacted cable in the joint area, but the total pressure drop per length across the joint is even less than in the regular CICC due to grooves machined in the CICC channel clam shells. Therefore, the joint does not represent any significant increase in impedance. Having this result, we made fabrication easier and less risky by modifying the CS design to decouple the joint from the helium outlet. That also removes the criticality of the joints and the outlet positioning in the CS, so we can move them within a range of several meters without noticeably affecting the symmetry of the flow in the CS module.

#### V. WELDING DEVELOPMENT OF THE JOINT

One of the critical operations of joint fabrication is restoration of the jacket around assembled joint. This feature

is similar regardless of the particular joint design. To weld the jacket back around the cable, we installed two clam shells joined by two butt welds and two longitudinal welds. For lower risk during fabrication, we chose to have the longitudinal welds on the vertical walls of the jacket.

The requirements for the welds came from structural analysis and from consideration of space allocation and the sensitivity superconducting strands to heat.

The welds need to be full-penetration type due to relatively high stresses. We analyzed stresses for different designs and were unable to find a better solution than a full-penetration joint.

Locating a full-penetration joint in the vicinity of the cable is risky because it may melt the strands and contaminate the weld or damage the strands by overheating them. Several mechanisms in addition to welding (e.g., by short overheating) can degrade superconducting strands. The most dangerous is melting the tin and generating high pressure inside the strand, which can damage the diffusion barrier and poison the copper matrix. That is applicable to internal tin strands only. The melting point of tin is about 232°C. Therefore, a conservative requirement often imposed on the maximum temperature in the cable during welding is 210°C.

In order to develop the welding procedure, we made two short mockup samples and one long sample with full-scale jackets.

#### A. First Weld Mockup Sample

We assembled a short piece of 316L material with 316L weld rod with TIG process, simulating a closeout weld piece, and instrumented it with thermocouples that were placed under the foil on the outer surface of the cable. In the areas where we instructed the welder to keep the temperature below 210°C, he had to make frequent stops, and even then, in the areas not protected by a backing strip or additional foil, the temperature excursion exceeded 500°C. After completion of the welds, we dissected the sample in many places and did metallographic studies that revealed poor fusion, crevices, and lack of penetration as a result of frequent stops. The test showed that it is very risky for structural purposes to try keeping the temperature under the weld below 210°C. The risk of a structural failure of the weld at the OD is by far greater than the risk of the superconductor damage by overheating.

Our earlier experience with the CS Model Coil showed that it is very difficult to keep the temperature low without maintaining a very high flow of compressed gas through the conductor, which would not be possible if the weld were a closeout weld. On the other hand, we observed during some SULTAN tests of ITER samples [4] that even intense damage of the strands on the OD of the cable does not reduce performance very much. We have plenty of margin in conductor performance near joint regions but not very much margin with regard to the structural safety. Therefore, the clear priority is to have a solid structure in the welds.

#### B. The Second Weld Specimen

In the second specimen, we modified the longitudinal welds in order to insert a backing strip. We also introduced an additional two layers of stainless steel foil on the top of the

cable under the butt weld in order to protect the cable from overheating.

We instructed the welder to lay a solid structural weld with low distortion and without trying to regulate the temperature.

After the weld was finished, we dissected the specimen to study the quality of the welds. Microstructural analysis showed a very-high-quality weld with full penetration and practically no defects.

#### C. Full-Scale Mockup of the Sintered Joint

In order to establish the final joint assembly procedure, close out welds, and observe the distortions during welding and after heat treatment, we built a 3 m long mockup sample that included all elements of the joint. After completion of the assembly and welding, we formed the joint to the radius of curvature corresponding to the outer radius of the CS module and took measurements. Because of the limited size of our R&D furnace, we made a three-wave sample instead of one single radius arc, as shown in Fig. 6. In order to make the shape registered, we installed fiducials on a sheet of plywood.



Fig. 6. Full-scale joint sample.

After heat treatment, we measured for deviation from the shape of the sample before heat treatment and discovered none. That is very useful information for CS fabrication; it showed that residual stresses did not get relieved during HT.

## VI. CONCLUSION

We qualified sintered and butt joints, including closeout welding. As a result of tradeoff studies, we selected a  $6 \times 6$  sintered joint for ITER CS interpancake joints.

## VII. ACKNOWLEDGMENTS

We are thankful to Laboratory Director Butch Irick and personnel at Magnet Development and to President Michael Coffey and personnel Cryomagnetics Inc. for their contributions to the fabrication and testing of the joints. We are thankful to Charlotte Barbier at Oak Ridge National Laboratory for her hydraulics computations.

## REFERENCES

- [1] N. N. Martovetsky, S.J. Kenney, and J. R. Miller, "Development of the Joints for ITER Central Solenoid," *IEEE Trans. Appl. Supercond.* 21(3): June 2011, pp. 1922–1925.
- [2] A. Di Zenobio et al., "Joint Design for the EDIPO," *IEEE Trans. Appl. Supercond.* 18(2): June 2008, pp. 192–195.
- [3] Technical Specification, ANNEX B, to Procurement Arrangement I.1.P6B.JA.01 between the ITER International Fusion Energy Organization and Japan Atomic Energy Agency, 2008, ITER IDM.
- [4] CRPP report, Assembly of USTF2 SULTAN Sample and Test Report, July 2008